Supporting Information for

The effect of surfactant concentration and aggregation on the growth kinetics of nickel nanoparticles

Alec P. LaGrow[1], Bridget Ingham[1,2], Michael F. Toney[3] and Richard D. Tilley[1]*

[1] The MacDiarmid Institute for Advanced Materials and Nanotechnology, Victoria University of Wellington, P.O. Box 600, Wellington 6140, New Zealand
[2] Callaghan Innovation Research Ltd., P.O. Box 31-310, Lower Hutt 5010, New Zealand
[3] Stanford Synchrotron Radiation Lightsource, 2575 Sand Hill Road, Menlo Park, CA 94025
* bridget.ingham@callaghaninnovation.govt.nz

S1. Rationale behind the SAXS fitting model used

S1.1. The use of the sticky hard sphere structure factor

The sticky hard spheres structure factor (describing inter-particle interactions) was chosen over the mathematically simpler hard spheres structure factor, because of the physical reasons behind the aggregation of particles. The hard spheres model describes a system where aggregation arises due to a high concentration of particles; however there are no preferred proximity relationships between the particles. In the sticky hard spheres model, particles experience an attractive ($u_0<0$) or repulsive ($u_0>0$) force in the neighborhood of another particle. In physical systems, this may be due to electrostatic, chemical or magnetic forces.

The sticky hard spheres structure factor uses four parameters: the hard sphere radius (R_{HS}), the perturbation parameter (ε), the 'stickiness' (τ), and the volume fraction (φ). The hard sphere radius is half of the minimum separation between the centers of two particles. It therefore cannot be smaller than the particle diameter. The attractive potential extends from $2R_{HS}$ to $2R_{HS} + \Delta$, and the magnitude of the attraction is given by the perturbation parameter $\varepsilon = \frac{\Delta}{2R_{HS} + \Delta}$ (see Figure S1). The model assumes ε is small, i.e. ≤ 0.1. The stickiness τ is related to the potential and ε by

$$\tau = \frac{1}{12\varepsilon}\exp\left(u_0 / kT\right)$$

.

The volume fraction is the volume of particles per unit volume in an aggregate of nanoparticles. Given that magnetism is the most probable source of attraction, it is reasonable to assume that τ and ε can be fixed to constant values for all samples and all scans at different times, since these describe the strength and range of the magnetic attraction between particles (vide infra).

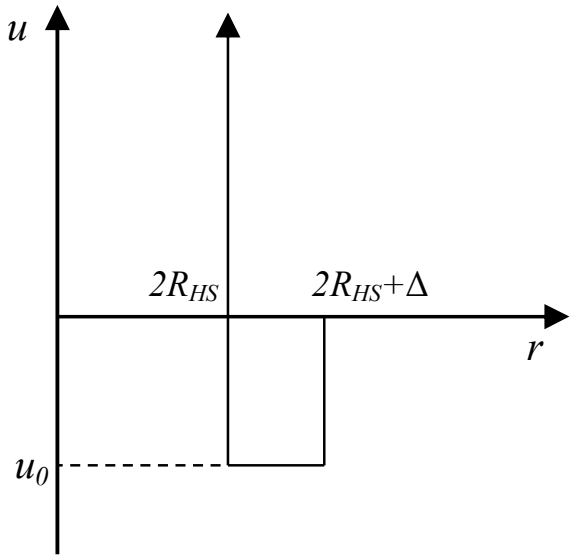

Figure S1. Diagram of the potential used in the sticky hard sphere structure factor model.

S1.2. Populations and parameters used

In total, four populations were used, with the following constraints to minimize the total number of parameters being fitted:

1. Low-q background: large scatterers to model Porod scattering background at low q ($I \sim q^{-4}$ dependence) - mean radius fixed at 1000 Å, dispersion fixed at 0.5.

2. High-q background: small scatterers to model slowly decaying background at high q - mean radius constrained between 5-10 Å, dispersion fixed at 0.5.

The need to include these 'background' populations is due to two factors. Firstly, large particles and aggregates may form over time with either broad scattering features (if these are polydisperse) or with scattering features at a low q outside the measurement range. Secondly, the background subtraction procedure is not completely adequate. Over the course of the reaction the viscosity of the solution decreases markedly (from a gel to a suspension). The X-ray transmission also varies throughout the experiment. This could not be measured in real-time, but only at the start and end of the reaction. All the data shown in Figure 1 have had the first scan subtracted, however the change in the solution properties, along with the change in transmission, means that this may not be completely sufficient, especially at later times. In any case, the additional scattering that may be introduced is expected to be a smooth function and can be approximated well by the addition of the two low-q and high-q populations described here. These two factors cannot be distinguished, but they have little impact upon the measurements of the primary particles observed (populations 3 & 4 below).

3. Non-interacting particles: spherical particles with dilute structure factor, i.e. non-interacting, S(q)=1.0.

4. Interacting particles: spherical particles using sticky hard spheres structure factor. The stickiness and perturbation parameters for the sticky hard spheres structure factor were fixed to 0.25 and 0.1 respectively. (The values used for the stickiness and perturbation parameters were obtained by comparing fits to different selected scans from different datasets, varying these values systematically over a physically reasonable range and observing the effect on the statistical parameters of the fit (χ^2). Several parameters appear to be highly correlated, e.g. τ, ε and dispersion.)

The volume fraction of particles in the aggregates will be higher than the average volume fraction throughout the solution. Therefore the 'interacting particles' population represents aggregated particles, while the 'non-interacting particles' population represents single particles in solution. We make the reasonable assumption that the size distributions for these two kinds of particles are the same, and hence the size distribution parameters (mean radius and dispersion) for these two populations were constrained to have the same value. For the experiment with TOP/Ni = 0.5 the distributions are broad and obtaining reliable values for the mean radius is difficult. The hard sphere radius, however, has lower uncertainty because it is inversely related to the position of the correlation peak. Therefore for this experiment, the mean radius was defined to be 2 nm less than the hard sphere radius, which is approximately the surfactant shell thickness.

This yielded a total of up to 9 parameters for each fit: total volume for all four populations, mean radii for populations 2 and 3, dispersion for population 3, and R_{HS} and φ for population 4. A list of all parameters used is given in Table S1. This was found to be adequate for all scans for all samples where TOP/Ni $\geq$ 0.5. An example of a 4-population fit to a dataset is shown in Figure S2.

Table S1. Populations and parameters used to fit the data in Figure 1.

	Population 1: low q background	Population 2: high q background	Population 3: non-interacting particles	Population 4: interacting particles
Volume distribution	Log normal: r_0 = 1000 Å σ = 0.5	Log normal: r_0 variable between 5 - 10 Å σ = 0.5	Log normal: r_0 variable σ variable	Log normal: $r_0 = r_0$ (pop3) $\sigma = \sigma$ (pop3)
Form factor	Spheres (no variable parameters)			
Structure factor	Dilute (no variable parameters)			Sticky hard spheres: τ = 0.25 ε = 0.1 φ variable R_{HS} variable
Number of variable parameters	1 (V_1)	2 (V_2, $r_{0,2}$)	3 (V_3, $r_{0,3}$, σ_3)	3 (V_4, φ, R_{HS})

For some of the samples, σ_3 was fixed or constrained to a maximum value of 0.3 (TOP/Ni = 1 and 2) or 0.4 (TOP/Ni = 0.5). In the case of TOP/Ni = 1 and 2, the dispersion values begin to increase rapidly once aggregation starts (Figure 5). Large values of dispersion result in broad scattering curves, so that the uncertainty on the fitted value of the dispersion is quite large. If the dispersion value was not constrained, the broadness of the feature effectively eliminated the relative sharpness of the correlation peak, so a maximum value for the dispersion of 0.3 was deemed to be acceptable. For the TOP/Ni = 0.5 case, the scattering patterns imply that the size distribution is somewhat broader, so the maximum value was

increased to 0.4. (Increasing to values higher than 0.4 did not change the fits significantly but resulted in greater variation in the other parameters.)

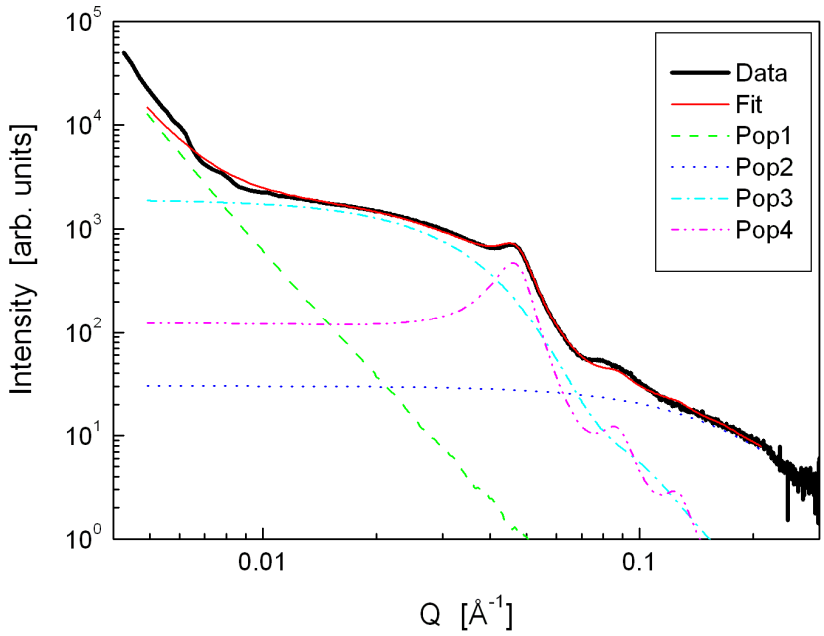

Figure S2. Example of a dataset from the TOP/Ni = 1 experiment (sample D in Figure 1) fitted with four populations, as described in the text.

S2. Fitted volume fraction

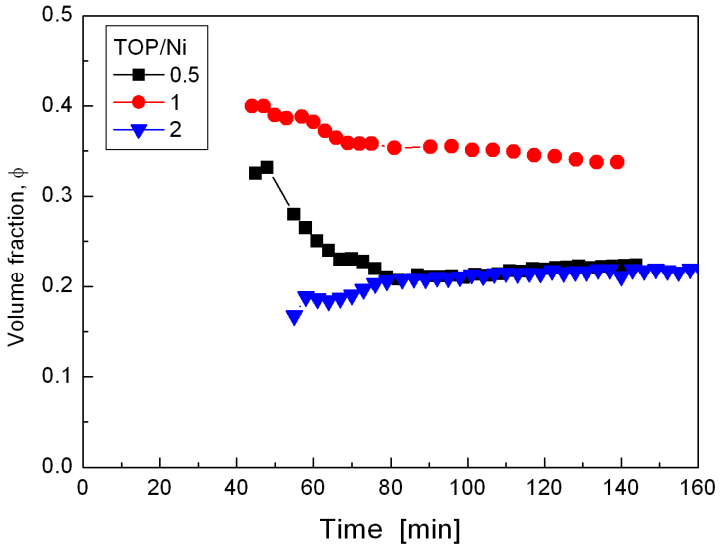

Figure S3. Volume fraction ϕ of particles in the aggregates for the Ni particle population 4.

S3. Alternative method for calculating rate constants.

For the case where $[A](t) < [A]_0$ and in the limit when $k_1 << k_2[A]_0$, equation 1 in the text can be linearized as follows:[35]

$$\ln\left[\frac{[A]_0 - [A](t)}{[A](t)}\right] = \ln\left[\frac{k_1}{k_2[A]_0}\right] + k_2[A]_0 t \qquad \text{(S2)}$$

Expressed in terms of volume $V_p(t)$, normalized to the maximum volume $V_{max} = [A]_0 M_w V_s / \rho$, equation S2 becomes

$$\ln\left[\frac{V(t)}{V_{max} - V(t)}\right] = \ln\left[\frac{k_1}{k_2[A]_0}\right] + k_2[A]_0 t \qquad \text{(S3)}$$

Fits of equation S3 to $\ln\left[\frac{V(t)}{V_{max} - V(t)}\right]$ are shown in Figure S4. The results for both fitting methods are compared in Table SII.

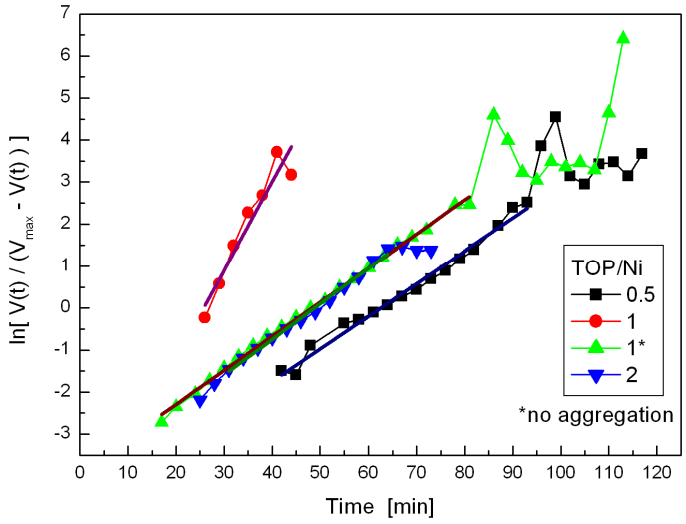

Figure S4. Fits to the total volume of particles versus time for various TOP/Ni concentrations as labeled, using equation S3.

Table SII. Rate constants fitted from curves in Figures 7 and S4.

	Using equation 3 (Fig. 7)		Using equation S3 (Fig. S3)	
TOP/Ni	k_1 (min^{-1})	$k_2[A]_0$ (min^{-1})	k_1 (min^{-1})	$k_2[A]_0$ (min^{-1})
0.5	0.0009 ± 0.0002	0.065 ± 0.005	0.0006 ± 0.0001	0.078 ± 0.003
1	0.00007 ± 0.00003	0.32 ± 0.02	0.0009 ± 0.0019	0.21 ± 0.03
1[a]	0.0019 ± 0.0001	0.076 ± 0.002	0.0016 ± 0.0001	0.0811 ± 0.0009
2	0.0011 ± 0.0003	0.100 ± 0.007	0.0013 ± 0.0002	0.085 ± 0.002

[a] Sample with no aggregation.

The sample with TOP/Ni = 1 which exhibited aggregation (D in the text) has quite different rate constant values obtained by both methods, compared to the other samples. This is partly related to the small number of data points available during the growth stage of the particles prior to aggregation (viz. Figure S4), and partly because the onset of aggregation and subsequent precipitation appears to be quite rapid, meaning that it is likely that V_{max} is underestimated in the fits of Eqn. 3 to the curve for this sample in Figure 7.

To estimate the possible spread of values that k_1 and $k_2.[A]_0$ might have for this sample, a series of curves akin to those shown in Figure S4 were produced from the data, using different values of V_{max}. The straight line plots, along with the corresponding curves related to the raw data, are shown in Figure S5, with the rate constants reported in Table SIII. This demonstrates that using a higher V_{max} for sample D gave rate constants (k_1) comparable to the results for samples C, E and F (Table SII). Therefore the value of k_1 given in Table I for sample D may be underestimated due to the small number of data points prior to the onset of aggregation and settling.

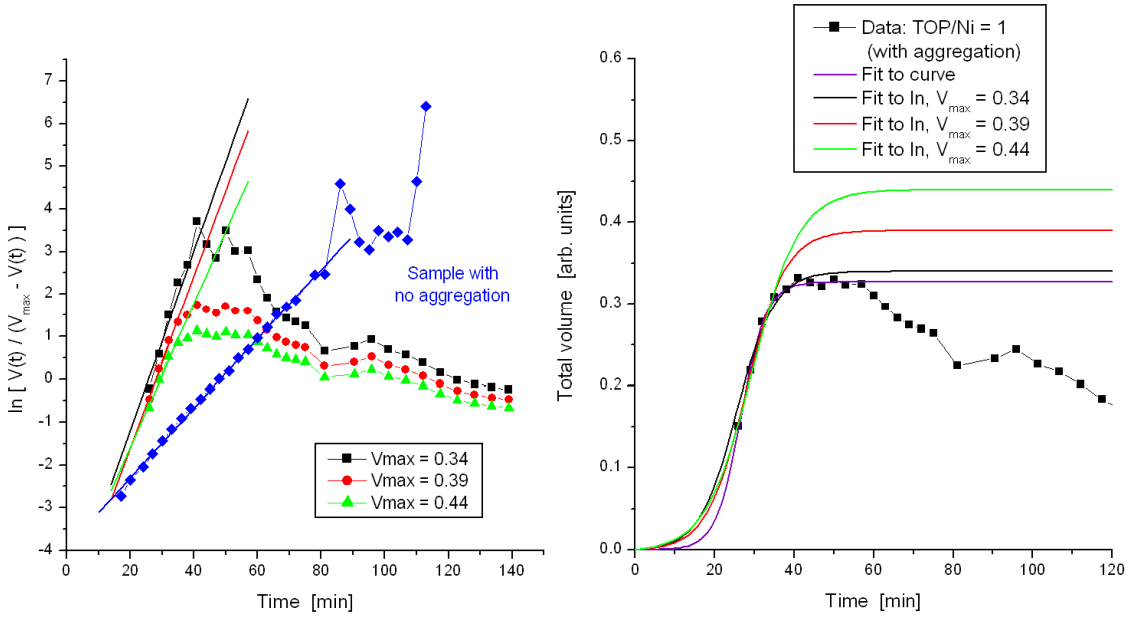

Figure S5. Left: calculated plots of the two TOP/Ni = 1 samples, with different values of Vmax for the sample showing aggregation, and the straight line fits from which the rate constants k_1 and $k_2.[A]_0$ are obtained. Right: calculated curves for the TOP/Ni = 1 sample with aggregation, using the values obtained from the straight line fits, compared with the raw data.

Table SIII. Rate constants from fitted curves in Figure S5 for the TOP/Ni = 1 sample showing aggregation.

V_{max}	k_1 (min^{-1})	$k_2[A]_0$ (min^{-1})
0.34	0.0009 ± 0.0019	0.21 ± 0.03
0.39	0.0007 ± 0.0005	0.20 ± 0.02
0.44	0.0012 ± 0.0010	0.17 ± 0.02
Eq. 3 (Fig. 7)	0.00007 ± 0.00003	0.32 ± 0.02